

EXPERIMENTAL AND NUMERICAL STUDY OF MOULDED WOOD TECHNOLOGY WITH FIBRE-PLASTIC COMPOSITE NODE ELEMENTS

Siavash Namari¹, Peer Haller¹

ABSTRACT: The reduction of CO₂ emissions and the enhancement of resource efficiency have emerged as significant motivators for research and development activities. One particular area of interest in sustainable building materials is moulded wood tubes, which offer the benefits of wood as a renewable resource and the material efficiency of composite construction. These tubes are well-suited for lightweight structures that are subject to dynamic and static loading. This paper proposes a method for joining thin-walled wooden elements with node elements composed of fibre-reinforced plastic (FRP) that incorporates integrally manufactured multilayer 3D fabrics that are adaptable to the component geometry. The investigation includes both experimental and numerical approaches to establish the load-bearing capacity of such connections. Experimental tests were conducted on specimens of different sizes under tension, while numerical models were developed to assess the load-bearing behaviour of small and large scale tests, as well as perform static verifications. The proposed solution has potential applications in the fabrication of a solar roof demonstrator. The results suggest that the use of FRP for connecting moulded wood tubes is a viable approach.

KEYWORDS: Connections, Composite structure, Moulded wood, Compressed wood, Fibre-reinforced plastics (FRP)

1 INTRODUCTION

The Federal Republic of Germany's industrial policy goals of reducing CO₂ emissions and enhancing resource efficiency have served as a catalyst for research and development efforts. These endeavours necessitate the utilization of sophisticated and expensive tools, but the structural mechanical performance remains suboptimal [1].

Besides the use of sustainable building material such as wood, the use of high-performance composite materials instead of traditional metallic construction materials is an efficient way of improving material and energy efficiency while decreasing carbon dioxide consumption. The potential of moulded wood technology in combination with fibre composite materials is particularly relevant in spatial structures which static systems primarily transmit normal forces. Recent studies have shown that the cellular structure of wood can be compressed under the influence of moisture and heat due to its thermo-hydro-mechanical properties [2]. This process is used by researchers to create moulded wooden construction elements formed from thin compressed wood panels, with a tubular cross-section being the simplest form. A tubular cross-section represents the simplest form, combining high structural strength for compression with very low material consumption [3]. Compared to massive solid wood cross-sections typically used in timber construction, moulded wooden tubes combine high structural strength for compression with very low material consumption, enabling a weight-efficient application of the material and saving up to 70% of the raw material [4]. Moulded

wooden tubes can be reinforced with high-performance fibres such as carbon or glass to create resource-efficient, high-performance composite wood components [5]. The positive properties of wooden tubes are especially useful in three-dimensional load-bearing structures, where compressive forces predominate due to the static system. These tubes have been used as rod-shaped construction elements in truss or lattice structures, including a 30m high truss structure built as a support for a 10kW wind power plant (see Figure 1) [6], [7].



Figure 1: Left: Moulded wooden tubes with reinforcements using glass, carbon or aramid fibres, Right: Wind power plant made of moulded wood tubes and steel connecting elements

Previously, steel joining solutions for construction required heavy castings or expensive, multi-step sheet metal forming. However, this project aims to develop a more efficient manufacturing and assembly process for lightweight timber construction systems. The paper will use moulded wood tubes and fibre-reinforced plastic composite as connection means, which are made of multilayer 3D fabrics. The adhesive connection of the node elements with the shaped wood profiles offers

¹ Siavash Namari, Peer Haller, Technische Universität Dresden (TU Dresden), Institute of Steel and Timber Construction, siavash.namari@tu-dresden.de

constructive advantages compared to mechanical fasteners, which imply a weakening of the cross-section. The combination of moulded wood and fibre-reinforced plastic enables versatile modular construction solutions that meet architectural and structural requirements. This innovative approach aims to remove the significant barriers to sustainable, lighter and architecturally diverse construction methods. After completion, a solar roof will be built as a technology demonstrator. The demonstrator will be characterized by high prefabrication, low dead weight with high load-bearing capacity and material efficiency. The construction should also be able to be implemented in a short assembly time. The final design is a pavilion with a roof made of solar modules that functions as a solar charging station, supported by two moulded wood elements (Figure 2).



Figure 2: Design of the technology demonstrator

Tensile testing has been performed on test specimens with varying geometries based on a design featuring 33, 25 and 17 cm long glass fibre-reinforced plastic (GRP) slats. These tests will be modelled using finite element method (FEM) software and compared against the test results. Subsequently, the demonstrator will be modelled in FEM software to showcase the performance of the lightweight wood support system. The load-bearing behaviour of the developed modules will be evaluated under site-typical load scenarios, providing valuable insights into their practical application. Any necessary design optimizations will be identified and incorporated accordingly. Ultimately, a comprehensive recommendation for structural implementation in lightweight timber construction support systems will be presented.

2 MATERIAL

2.1 Thermo-Hydro-Mechanical Treatment

In mechanical wood technology, it is well known that low strength and durability can be improved by treatment with increased temperature and humidity. These processes are known as Thermo-Hydro-Mechanical (THM) processes. Under THM conditions, the amorphous building blocks of the wood structure soften, which enables shaping, compression and bending. The viscoelastic behaviour of the wood is utilized, whereby at low temperatures and low moisture content, the wood behaves like glass, while at high temperatures and high moisture content, it shows entropy-elastic behaviour.

Thermo-hydro-mechanical compression can reduce the cavities in the wood cells, especially in hardwood. Theoretically, wood can be compressed in all directions (longitudinal, tangential, or radial), but compression in the radial direction is the most practical. Due to the porous cell structure, it is possible to contract the cell structure in the compression process with an appropriate process regime without causing microscopic damage to the cell structure. The process of compressing wood typically occurs in a hot press with a constant displacement rate at high temperatures ranging between 120 to 160 °C. If the press is opened immediately after the compression process, compressed wood (CW) may exhibit partial springback or return to its original shape. To counteract this, it is necessary to cool the CW specimens down to below 80 °C while in the compressed state. Post-treatment may be required subsequently to limit this effect and ensure dimensional stability. Recovery, a characteristic of CW whereby it achieves partial or complete recovery of its original dimensions when exposed to water or high humidity, is known as shape memory. In this project, to avoid CW springback, specimens were cooled to 40 °C after compression, thereby ensuring stable dimensions. The research results show that CW and CW connectors offer a significant increase in the strength and stiffness properties compared to normal softwood or hardwood [8].

2.2 Moulded Wood Production

Wood has numerous advantages as a building material, including its eco-friendly properties and environmental friendliness. While wood performs well in most areas, some materials may outperform it in terms of specific properties such as density and Young's modulus. To make the most of wood as a building material, it is crucial to consider both its advantages and disadvantages. For example, wood has lower strength, is anisotropic and is vulnerable to weathering [9]. To maximize wood's positive attributes, it is often used in combination with other materials such as steel, concrete, glass and textiles in sustainable construction methods. Softwood is the most commonly used type of wood in construction because of its straight, long trunks. The development of moulded wood technology also opens up new possibilities for using deciduous trees in construction, contributing to a more sustainable building industry.

In addition to mechanical properties, the structural and economic performance of a cross-section is also important. The sawmill, as the primary step in the value-added chain, plays a crucial role in the provision of full cross-sections from a grown tree. However, the process results in significant material losses and a lack of competitiveness, as only about 60% of the stem wood remains of value [10]. To improve efficiency, material savings must be made during cross-section formation. The yield of raw wood and waste significantly affect the price structure of wood products, favouring tree species with long and straight trunks, such as softwoods like spruce, over hardwoods with branched crowns like beech or oak. The manufacturing of rectangular cross-sections involves traditional machining methods, including sawing, milling,

planning and sanding with minimal energy and force, followed by joining with synthetic binding agents. The use of round and rectangular solid cross-sections in wood-based materials is commonly accepted in the construction industry [9]. However, compared to other technical profiles made of metal or plastic, the full cross-sections created by traditional processing methods have a lower second-degree moment of Inertia. The compression process creates deformation reserves in the wood, which are later used for bending. With a suitable process regime, depending on temperature, humidity and compression speed, the compression process is reversible and fixable with almost no damage to the cell structure. The compression direction runs in the plane of the plate. In the subsequent moulding process for the production of thin-walled tubular cross-sections, the solid wood panel is shaped into profiles with the addition of heat and moisture and then fixed, as can be seen in Figure 3.

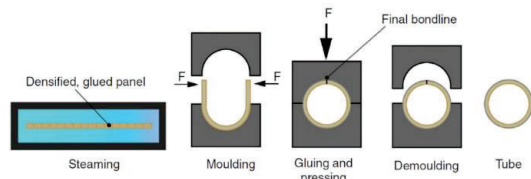


Figure 3: Schematic production of a wooden tube by shaping [11]

The ability of cell walls to recall memory means that the folding is reversible and the radius of curvature of the moulded wood tubes depends on the intensity of the previous compression. All open and closed profile shapes with any length and thickness can be produced using this technique. The successful process for manufacturing moulded wood profiles is patented by the Technical University of Dresden. The numerous investigations and derived properties of the moulded wood profiles have shown decisive advantages, including a lower weight compared to the full cross-section, small shrinkage, the use of all types of wood, including deciduous wood of lower quality, low waste in the sawmill, forming instead of machining and the high synergy of the bond with fibres. Product-specific evaluations in comparison with sawn, glued and glued laminated timber have demonstrated the technology's biggest advantages.

2.3 Fibre-Plastic Composite Node Elements

As mentioned, this paper aim to develop new node elements for lightweight structural systems made of moulded wood elements. The aim is to ensure a correct and constructive connection between the moulded wood profiles to transfer stresses caused by load between them. The node elements will be produced from multi-layer fabric and resin systems. Previous material models will be used to calculate the material parameters and the appropriate polymeric resin of the matrix will be selected based on simulations.

The fibre-reinforced plastic node elements offer a multitude of advantages over existing metal connections. For successful use in lightweight support systems, the

advantages must be put into practice. The decisive advantages are, among other things, the significantly reduced weight of a node element made of fibre plastic compared to steel alternatives and the resulting lower assembly effort due to the unnecessary use of heavy equipment. This results in the possibility of realizing new supporting structures. A symbolic node element is shown in Figure 4.



Figure 4: Node element made of carbon fibre [12]

The connection of moulded wood profiles with fibre-plastic composite node elements is a relatively new field and as such, there is no established calculation method to evaluate the material behaviour of the structural adhesive connection. Therefore, previous material characteristics of glued wooden surfaces must be adapted to the structural adhesive connection. The load-bearing capacity of a structural adhesive connection primarily depends on the shear and transverse tensile stresses occurring in the adhesive surface.

3 EXPERIMENTAL PROGRAM

3.1 Material and methods

The aim of these tests was to use force-displacement diagrams to quantify the load-bearing behaviour and characterize the failure mechanisms. Proportionally reduced test specimens were produced for the uniaxial tensile test and three different test specimen series with different dimensions were produced. Spruce glued laminated timber compressed by around 25% was used as the material and five test specimens were produced per series.

The test specimens were designated according to the length of the lamination and the GRP lamellae. The designation of the test specimen of GRP-H33 shown in Figure 24.

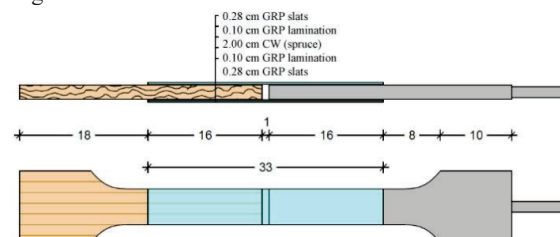


Figure 5: Test specimen GRP_H33

Tensile test specimens made of compressed spruce wood, fibreglass lamination, Plexus MA300 adhesive and two Glass Reinforced Plastic (GRP) lamellae. The test

specimens were assembled by sanding and applying a spacer and an adhesive layer, followed by the GRP lamella set. The elastic adhesive connection was used to absorb tensile shear loads that primarily occur in the tensile test. Three different test series with different dimensions were produced for the tensile tests. The results were evaluated based on the force-displacement diagrams.

Table 1 summarizes the properties of the materials used in the test specimens, including the density, tensile strength and Young's modulus of the compressed wood, glue and GRP.

Table 1: Properties of the materials of the test specimens

Characteristic	CW	Glue	GRP
density ρ [g/cm ³]	0.61	0.97	1.76
tensile strength R_m [N/mm ²]	55.9	20.7-27.6	319
Young's modulus E [N/mm ²]	15600	931-1137	20500

The tensile test was conducted at room temperature of 20°C and 65% relative humidity, in accordance with ISO 554:1976-07 and The test run corresponds to the loading procedure DIN EN 26891:1991-07. The test setup, involved hanging the test specimens in the testing machine with a steel connector. The ALMEMO 2890-9 precision measuring device and data logger, together with two displacement sensors, were used to measure the applied force and displacement.

3.2 Experimental setup and results

The samples showed a linear load-displacement behaviour until sudden and brittle failure of the fibre reinforcement and wood cross-section, with the specimens failing at an average load of 65 kN.

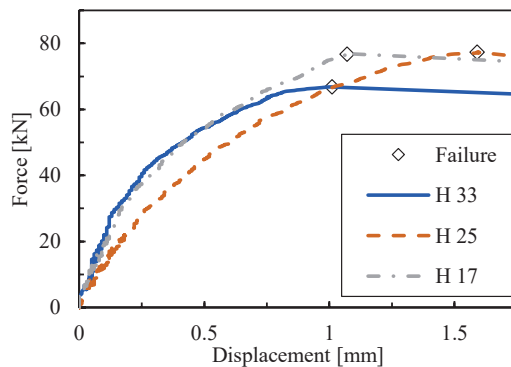


Figure 6: Force-displacement diagram for the tensile test series

Test series consists of three test bodies with GRP lamellae of different lengths, one for each previously described test body series. Table 9 summarizes all relevant properties of the test body series for the main conclusions, with values obtained from the mean values of all considered test specimens. The maximum load is greater for the test specimen series with a GRP lamella length of 25 cm, while the displacement is larger for the 33 cm specimens

with wooden components. The steel component values have only marginal differences. The smallest displacements at the highest possible maximum loads are achieved for the test specimen series with a GRP lamella length of 17 cm. Although the maximum load and displacement are of secondary importance due to the different test specimen geometries, the expected maximum load of 55.9 kN is exceeded for all test specimen series with wooden components, indicating that the wooden body has a higher tensile strength in the composite.

Table 2: Maximum loads, displacements of the test series

Test specimen	H 33	H 25	H 17
F_{max} [kN]	64.79	77.48	73.79
u_{max} [mm]	1.24	1.45	1.05
k_s [kN/mm]	85.50	78.44	99.60

The displacement modulus, denoted as K_s , is a measure of the stiffness of a timber connection and is used to assess its load-bearing capacity and serviceability. It represents the force required to produce a displacement of 1 mm. The DIN EN 26891:1991-07 test procedure is used to determine the displacement modulus for mechanical fasteners. However, since there is no standard for adhesive connections in Euro code 5, this procedure is also used to evaluate the stiffness values of adhesive wood connections, enabling comparison of the test specimens' stiffness values. For mechanical fasteners, the displacement modulus is determined by the load application, structural conditions, connection type, load-bearing capacity and accuracy of fit, characterizing the displacement of the fastener. However, for adhesive connections, determining the displacement modulus is more challenging as it depends on the displacement of the entire adhesive surface and, therefore, the test specimen. The force-displacement relationship is used to derive the stiffness of adhesive connections.

Four different failure modes were identified, with the failure of the lamination being the most critical. For the failure of the lamination, two different failure modes were observed: either the lamination detaches from the wood surface or the wood-side lamination detaches from the adhesive bond but remains attached to the wood surface. The exact differentiation between these two possibilities is not possible due to the overall failure of the lamination. Another type of failure is the breakage of the GRP lamella, which mainly occurs at the connection to the steel member and occurs both vertically and horizontally. The failure of the splice and the fracture of the wooden body are also observed. The irregular fractures of the wooden specimens can be due to irregularities in the wood or knots. Figure 7 shows an example of the failure mechanism of the tensile test.

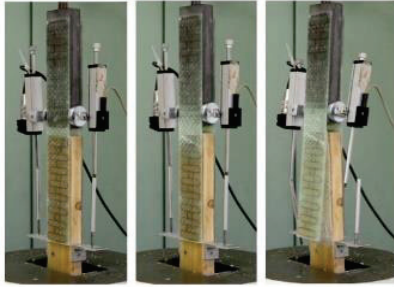


Figure 7: An example of failure mechanism of tensile test

The lamination failure is evident in almost every test specimen and can be identified as a critical failure. In the test specimen series H33, the failure of the GRP lamella is also identified for all test specimens. There are occasional breaks in the wooden body across all series, but failure mode (d) is not decisive.

For all test specimens of the series with steel components, the breakage of the GRP lamellae is recognizable as the decisive failure. The failure of the adhesive connection only occurs once and can be explained by the insufficient processing of the adhesive and the resulting weak points. In summary, while the lack of video recordings makes it difficult to fully understand the failures, the images of the test specimens allow for the assessment of the relevant failure mechanisms. The failure of the lamination and the breakage of the GRP lamellae are identified as the critical failures.

4 NUMERICAL MODEL

The modelling of wood is a complex and challenging task due to the many structural parameters and the variable environmental conditions that influence the mechanical properties of the material. Moisture, in particular, has a significant impact on the mechanical behaviour, along with the type of load, duration and temperature. Natural features such as density, knots, aging and orthotropic also affect the material properties.

For Finite Element Method (FEM) models, no universal model exists that can fully and precisely describe the constitutive relationships of wood. Different models and approaches are used, depending on the type of problem to be solved. Fracture mechanics approaches are used for brittle problems, while a combination of the classical flow theory of plasticity with a criterion according to Hill, Hoffman, or Tsai-Wu is used for ductile problems. Physical, mathematical-static and hybrid model approaches can also be used and simplifications related to damage and failure may be applied to ensure reliability.

This article focuses on a mathematical-static model, which has a high degree of reliability but limited scope. The material properties used in the model are selected based on the load and are divided into the elastic range, the transition from elastic to plastic with the associated yield condition and the plastic range with the hardening law. According to the theory of material behaviour modelling, there are four essential building blocks for creating a reliable model. These include a valid material

model, loading condition, a hardening law and reliable material data [13]. However, modelling materials realistically can be challenging due to various factors. For instance, the yield surface only describes the moment when failure occurred but not the type of failure.

Despite these difficulties, the approaches described serve as a simplified assumption for understanding the material behaviour and subsequent finite element (FE) modelling. Modelling wood as a material is a complex subject influenced by various factors such as moisture, viscoelasticity and so on in addition to elastic and plastic deformation [13]. The ANSYS software, which is a finite element software used to solve linear and nonlinear problems in structural mechanics, is employed to model tensile tests and later the demonstrator. The simulation process used an extensive trial-and-error method until the simulation results matched the experimentally performed tensile tests.

4.1 Material Parameters

The materials of the components and their properties are defined in the technical data. The material properties of the GRP slats are taken from the material data sheet provided. The density, modulus of elasticity and maximum tensile strength are given and a bilinear isotropic hardening model is selected. The yield point and tangent modulus are required to characterize the bilinear isotropic hardening, but there is no data for either property, so assumptions were made and continuously improved during the simulation process. The values summarized in Table 10 are assumed as material properties.

Table 3: Material properties of the GRP slats

Characteristic	Value	Unit
density ρ	1760	kg/m ³
Young's modulus E	20500	MPa
Poisson's ratio ν	0.18	-
bulk modulus K	10677.08	MPa
shear modulus G	8686.44	MPa
Stretch limit R_p	75	MPa
tangent modulus E_T	8000	MPa
Max Tensile Strength R_m	319	MPa

Similar to the GRP slats, the lamination of wood is made up of a fibre material and resin. The material properties are summarized in Table 4

Table 4: Material property of the lamination of the wood

Characteristic	Value	Unit
density ρ	1760	kg/m ³
Young's modulus E	18000	MPa
Poisson's ratio ν	0.18	-
bulk modulus K	9375	MPa
shear modulus G	7627.12	MPa
Stretch limit R_p	65	MPa
tangent modulus E_T	5000	MPa
Max Tensile Strength R_m	250	MPa

The wood component of the test specimen consists of compressed spruce wood with a degree of compression V of about 25%. Due to the orthotropic, the orthotropic elasticity is used with three Young's modules, Poisson's ratios and shear moduli. The same values are used for the values in the tangential and radial directions, as these differ only minimally in the specified directions and only the properties perpendicular to the fibre were determined in the tests.

Table 5: Material properties of the compressed wood ($V = 25\%$)
(Sources: [8]; [14]; [15])

Characteristic	Value	Unit	Ref.
density ρ	610	kg/m ³	[8]
Young's mod. Long. E_L	770	MPa	[8]
Mod. elasticity radial E_R	770	MPa	[8]
Mod. elasticity tang. E_T	15600	MPa	[8]
Poisson's ratio ν_{RT}	0.43	-	[14]
Poisson's ratio ν_{TL}	0.025	-	[14]
Poisson's ratio ν_{RL}	0.04	-	[14]
shear modulus G_{RT}	50	MPa	[15]
shear modulus G_{LR}	840	MPa	[8]
shear modulus G_{LT}	840	MPa	[8]
compressive strength $f_{c,L}$	66.7	MPa	[8]
compressive strength $f_{c,R}$	7.5	MPa	[8]
compressive strength $f_{c,T}$	7.5	MPa	[8]
tensile strength $f_{t,L}$	55.9	MPa	[8]
tensile strength $f_{t,R}$	0.5	MPa	[8]
tensile strength $f_{t,T}$	0.5	MPa	[8]
shear strength τ_{LT}	8.8	MPa	[8]
shear strength τ_{RT}	8.8	MPa	[8]
shear strength τ_{LR}	8.8	MPa	[8]
Stretch limit R_p	55.9	MPa	-
yield stress ratio R_{11}	1	-	-
yield stress ratio R_{22}	0.11	-	-
yield stress ratio R_{33}	0.11	-	-
yield stress ratio R_{12}	0.23	-	-
yield stress ratio R_{13}	0.23	-	-
yield stress ratio R_{23}	0.23	-	-

In the model used here, the mesh for all 8 components of the test specimen consists of tetrahedrons, as this was the only way to find a solution due to the geometry of the shoulder stick shape used and the size of the mesh.. Overall, the geometry shown in Figure 8 is meshed with 8938 elements and 20657 nodes.

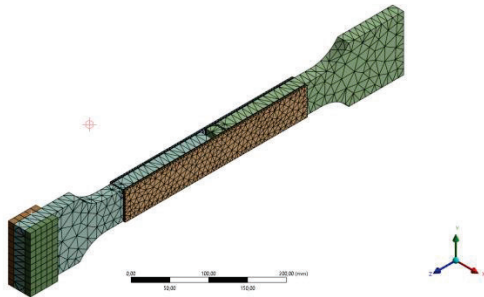


Figure 8: Meshed geometry of the tensile sample

4.2 Comparison of the numerical and experimental results

With the described material and simulation parameters, as well as mesh refinement, the force-displacement diagram shown in Figure 9 was obtained. This diagram shows all curves of the tests and the ANSYS model. The model curve is almost identical to that of the tests.

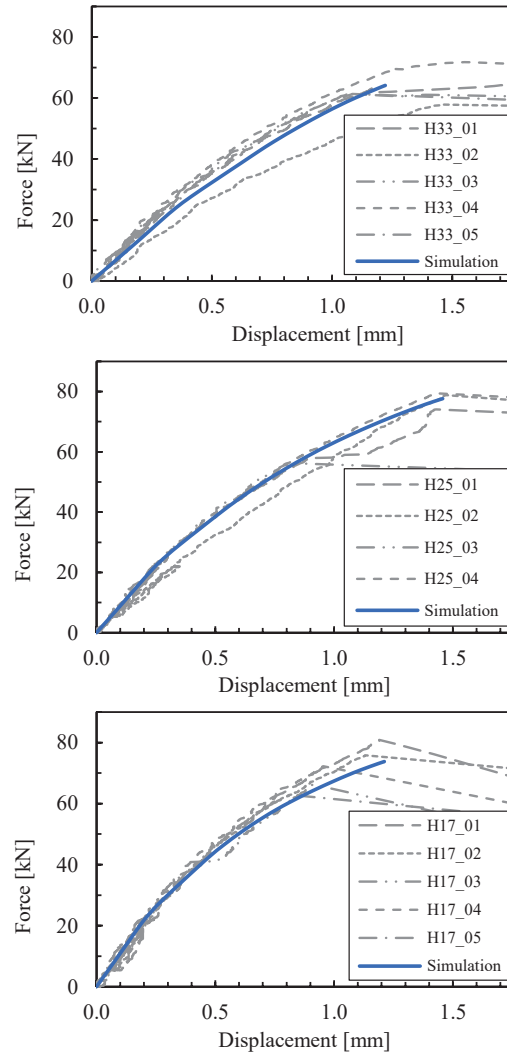


Figure 9: Comparison of the force-displacement diagrams of test specimen with the numerical model

For the model of the test specimen with a GRP length of 33 cm, the yield strength of the of the wood was set at 66 MPa based on the test data. To evaluate the model further, the displacement modulus of the tests is compared with that of the model. The displacement modulus is evaluated similarly to the calculation of the displacement modulus of the tests. For a direct comparison, the displacement modulus is evaluated analogously to the expected maximum load of 55.9 kN of the tests.

Figure 10 shows the maximum main stresses of the entire component. The principal normal stress hypothesis is used to predict the failure of brittle materials without yielding.

Positive values indicate tensile stresses and negative values indicate compressive stresses. The highest tensile stress is 305.01 MPa and the highest compressive stress is 59.64 MPa. The exact locations of the maximum stresses are evaluated separately and the GRP lamellae in the transition area from wood to steel components have the highest stress values on the surface.

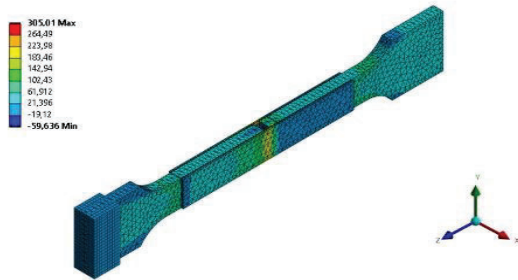


Figure 10: Maximum principal stresses (MPa) of the entire component H33

Figure 11 shows the maximum principal stresses of the wood components, which are analysed separately as the weakest part of the composite. Due to the lack of damage in the model, the tensile stresses in the model are compared with the maximum tensile strength or yield point.

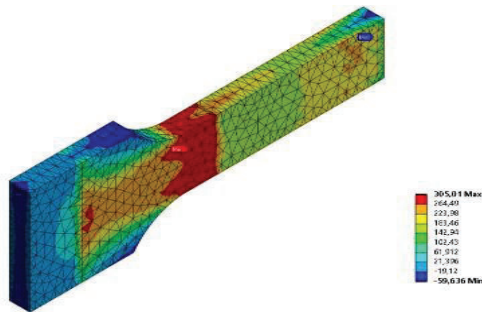


Figure 11: Maximum principal stresses (MPa) of the timber member H33

In the positive Z-direction, the maximum stresses over the entire cross-section develop into two stress peaks, which are illustrated in Figure 12. The crack of test specimen 02 of the test specimen series H33 is shown. It is located exactly where the curve of the shoulder stick shape begins and coincides with the edge of the red area of the stress distribution. The maximum tensile stress within the wood component is 66.4 MPa, which exceeds the material's specified yield strength of 66 MPa, causing the wood component to fail.

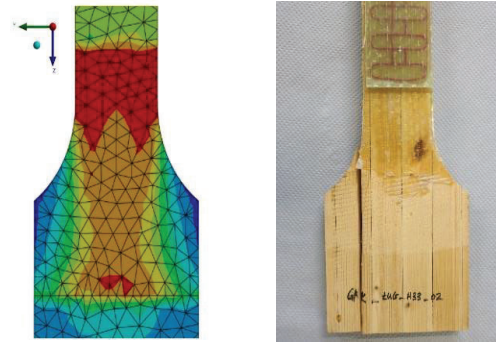


Figure 12: (left) Stress distribution of the wood on the shoulder stick shape H33, (right) Fracture of the wooden body of the test specimen H33

Figure 13 (left) shows the stresses curve in the horizontal direction, while Figure 13 (right) shows it in the vertical direction, with the cutting plane at the level of the maximum value. The greatest tensile stress was found to be within the steel component at the edge of the lamination layer.

However, the theory of maximum principal stress only applies to brittle materials and the steel component is the only component exhibiting ductile material behaviour. Therefore, the values of the maximum tensile stresses on the steel component must be interpreted with caution. Furthermore, the stress must be treated with care due to the high stress gradient in the direction of the negative X-axis.

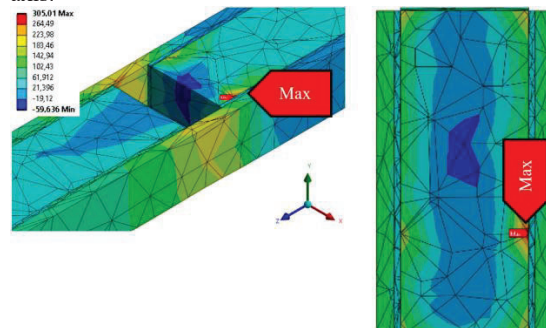


Figure 13: (left) Stresses in the horizontal section plane H33, (right) Stresses in the vertical section plane H33

Comparing the stress distribution of the maximum tensile stresses in the wood component and the adjacent slats provides insight into an optimal GRP slat length. The lamellas in the three models show the highest tensile stresses, with decreasing lamella length resulting in an increase in stress despite lower maximum loads. The stress distribution in the wooden component is similar in all models, with stresses increasing from the middle of the test specimen to the end of the GRP lamella.

5 Model of the Demonstrator

The demonstrator will consist of circular-shaped wood profiles and fibre-reinforced plastic node elements. The purpose of this modelling is to evaluate the performance

of the fibre-reinforced load-bearing systems made of wood.

The purpose of the demonstrator is to showcase the aesthetics and performance of moulded wood profiles reinforced with fibre-reinforced plastic node elements, while also serving a practical function. As a result, the building must meet certain construction requirements. To meet these requirements, a pavilion was built with a high enough roof to allow for space underneath and with solar modules as the roof to allow for the generation of solar energy. This energy could then be used to power a charging station for electric bicycles or scooters while also protecting them from the weather.

The pavilion was designed with a bar structure supported by two moulded wood supports that are 3 meters apart, with the node profiles fixed symmetrically to the supports for both sides. The roof was initially planned as an inward sloping barrel roof with innovative curved solar modules, but due to issues with module procurement and unpredictability, the roof shape was changed to a straight through roof. The roof has a surface area of 4.95 meters in length and 3 meters in width, with a one-sided inclination of 3° to ensure water drainage. The solar modules are attached to the edge and centre rails using different aluminium profiles, which are then connected to the moulded wood profiles via steel plates negligible.

The moulded wood supports have a circular ring cross-section with an outer diameter of 23 cm and a wood thickness of 2 cm. The branches connected to the supports have the same dimensions for both supports, with the lower branch connecting to the support at an angle of 55° and a maximum length of 2.022 meters. The upper branch is at an angle of 65° to the support and is 1.788 meters long. The node elements are identical for both columns, with a height of 37.2 cm and a gap between the elements. The materials used in the model include moulded wood profiles for the supports and branches, fibre-reinforced plastic for the node elements, steel for the edge and centre supports and aluminium for the edge and middle rail. Glass was used for the roof construction, with a high modulus of elasticity of 70,000 MPa and a density of 29.85 kg/m^3 . The load-bearing behaviour of the wood profiles would be improved with lamination for protection against the weather, but this was not modelled. The calculation model developed for the demonstrator is based on the reliable orthotropic material properties of the wood determined by compression tests on moulded wood pipes. The model assumes an ideal bond between the wood and fibre-reinforced plastic.

The models were based on six possible wind load positions and their respective load combinations. Due to the large number of models and the similarity in the truss structure's behaviour under load, not all models are described. It was observed that a two-sided wind load, regardless of the direction of action, had a more favourable effect on the entire supporting structure than a one-sided load. Due to the loading on both sides, the deformations in the upper and lower branches of the columns were of the same magnitude on both sides. The composite roof had a stiffening effect that prevented

major deformations on both sides. The deformations were specified separately for each direction of the coordinate system and Figure 14 provided an overview of the order of magnitude of the total deformation of the demonstrator, showing that the greatest deformations were in the centre of the roof area. The low deflection when the load was introduced at a point indicated that the roof construction was very stiff and could be neglected for the evaluation.

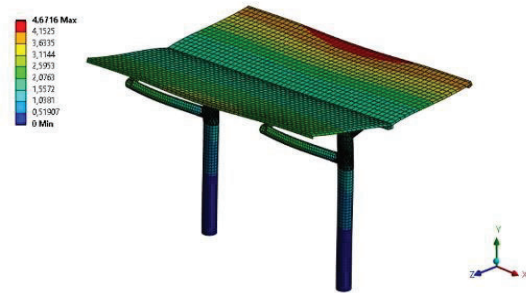


Figure 14: Total displacement of the model with the load position bilateral wind pressure

The deformation behaviour of the construction differs between wind pressure and wind suction. Under two-way wind suction and load combination 1, which results in a total uplift load, the structure is displaced in the negative X-direction, while under two-way wind suction the displacement takes place in the positive X-direction. This deformation behaviour can be explained by the longitudinal roof pitch. The normal vector of the wind load points in the same direction as the resulting displacement. Under wind suction, the upper and lower branches deform in the Z-direction in the same amount. Both are pulled upwards as a result of the suction. Under wind pressure, the lower branch deforms more than the upper branch due to its greater length.

The serviceability limit state was checked using the displacements. In order to be able to assess the ultimate limit state, a stress evaluation is required. In the models with wind pressure loading, the largest tensile and compressive stresses occur at the same location. Both maximum values are reached on the inside in the rear upper node element (Figure 15).

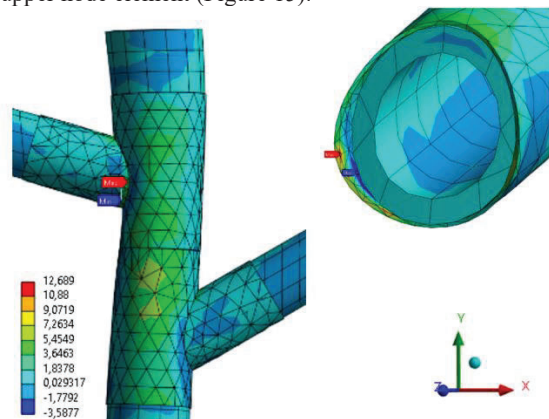


Figure 15: Maximum principal stresses in model 1 (values in MPa)

All tensile and compressive stresses that occur in the models are significantly lower than the maximum strengths of the individual materials of the components. The demonstrator model results show that the truss structure is stable enough to withstand maximum external loads.

The deformation behaviour of the bar structure is accurately represented and the maximum displacement values are within permissible limits. The stress evaluation of the supporting structure is consistent with the expected stress distribution and heavily stressed areas. Stress levels in the model are relatively low, but the roof structure has a significant impact on the load-bearing behaviour of the truss structure.

6 CONCLUSIONS

In this paper, the importance of advancing innovative constructions in timber technology was emphasized. While wood has clear advantages in construction, it also has technical limitations that must be addressed. The development of moulded wood profiles has demonstrated great potential for use in architecture, construction, lightweight construction and plant construction, as it improves weak points in technical applications of wood. Additionally, the use of technical fibres and textiles has increased efficiency and lowered material costs in timber construction. The combined use of moulded wood and fibre-reinforced plastics is developed coherent and modular construction solutions that meet a variety of architectural and structural requirements and enable a broad range of applications.

Test programme and the numerical models are being used in an attempt to provide sound knowledge for moulded wood tubes connecting with fibre-plastic composite node elements. The lightweight wood construction system developed features a high degree of prefabrication, extremely low dead weight with high load-bearing capacity, material efficiency and durability. Based on the moulded wood technology, a technology demonstrator in the form of a solar roof will be built.

In summary, the models used in this study were found to reliably represent tests to failure, despite simplifications and idealizations. Results of tensile tests showed that mechanical properties of wood components can be improved in combination with fibre-reinforced plastics, particularly in terms of optimal lamella length. The joining technology of shaped wood profiles and node elements using adhesive technology was found to offer an optimally adaptable force transmission surface, which is an advantage over mechanical connection means. Further testing is needed to ensure functionality under fluctuating mechanical loads and climatic conditions.

ACKNOWLEDGEMENT

The authors gratefully acknowledge the funding provided by the ZIM via Federal Ministry for Economic Affairs and Climate Action of Germany. The authors also thank the project partners Institute of Textile Machinery and High Performance Material Technology of TU Dresden,

Korropol GmbH and Niemeier Fahrzeugwerke GmbH for their collaboration.

REFERENCES

- [1] F. M. o. F. (Germany), „Immediate climate action programme for 2022,“ 2022. [Online]. Available: <https://www.bundesfinanzministerium.de/Content/EN/Standardartikel/Topics/Priority-Issues/Climate-Action/immediate-climate-action-programme-for-2022.html>. [Zugriff am 2023 02 01].
- [2] G. F. Navi P, „Effects of thermo-hydro-mechanical treatment on the structure and properties of wood,“ *Holzforschung*, pp. 287-293, 2000.
- [3] J. Hartig, J. Wehsener und P. Haller, „Experimental and theoretical investigations on moulded wooden tubes made of beech (*Fagus sylvatica* L.),“ *Construction and Building Materials*, 2016.
- [4] J. Wehsener, T. Werner, J. Hartig und P. Haller, „Advancements for the structural application of 19 fiber-reinforced moulded wooden tubes,“ *Materials and Joints in Timber Structures*, Springer, Nr. 20, pp. 99-108, 2014.
- [5] P. Haller, „Concepts for textile reinforcements for timber structures,“ *Materials and Structures*, Nr. 40, p. 107–118, 2007.
- [6] T.-E. Werner, „Profil aus Holz und Verfahren zu seiner Herstellung“. Germany Patent 102007015018A1, 2007.
- [7] B. Hahn, T. Werner und P. Haller, „Experimental and numerical investigations on adhesively bonded,“ *Construction and Building Materials*, 2019.
- [8] S. Namari, L. Drosky, B. Pudlitz, P. Haller, A. Sotayo, D. Bradley, S. Mehra, C. O’Ceallaigh, A. M. Harte, I. El-Houjeiry, M. Oudjene und Z. Guan, „Mechanical properties of compressed wood,“ *Construction and Building Materials*, 2021.
- [9] P. Haller, *Structural wood engineering handbook*, 2009: Verlagsgesellschaft Rudolf Müller, Stuttgart.
- [10] P. Haller, A. Ringhofer und G. Schickhofer, „Wood, timber and structural elements: economic, mechanical and technological aspects,“ *Wood Material Science & Engineering*, pp. 261-267, 2015.
- [11] A. Kuntar, D. Sandberg und P. Haller, „Compressed and moulded wood from processing to products,“ *Holzforschung*(, Nr. 7, p. 885–897.
- [12] ITM, „Institute of Textile Machinery and High Performance Material Technology,“ 03 29 2022. [Online]. Available: <https://tu-dresden.de/ing/maschinenwesen/itm>.
- [13] P. Niemz und W. U. Sonderegger, *Eigenschaften, Prüfung und Kennwerte*, Hanser, 2021.

- [14] R. Ross, Wood handbook: Wood as an engineering material, U.S. Department of Agriculture, Forest Service., 2021.
- [15] C. Sandhaas, Mechanical behaviour of timber joints with slotted-in steel plates, Wöhrmann, 20212.